
Article:
Suen, KM, Lin, CC orcid.org/0000-0003-3071-172X, Seiler, C et al. (6 more authors) (2018) Phosphorylation of threonine residues on Shc promotes ligand binding and mediates crosstalk between MAPK and Akt pathways in breast cancer cells. International Journal of Biochemistry and Cell Biology, 94. pp. 89-97. ISSN 1357-2725

https://doi.org/10.1016/j.biocel.2017.11.014

Phosphorylation of threonine residues on Shc promotes ligand binding and mediates crosstalk between MAPK and Akt pathways in breast cancer cells

Suen KM[†1,2,8], Lin CC[†3], Seiler C[3], George R[4], Poncet-Montange G[5], Biter AB[6], Ahmed Z[1], Arold ST[7], Ladbury JE*[3]

[1] Department of Biochemistry and Molecular Biology, and [2] Graduate School of Biological Sciences, The University of Texas MD Anderson Cancer Center, Unit 1954, 1515 Holcombe Blvd, Houston, TX 77030, U.S.A.

[3] School of Molecular and Cellular Biology, University of Leeds, LC Miall Building, Leeds, LS2 9JT, U.K.

[4] Structural Biology STP, The Francis Crick Institute, Lincolns Inn Fields Laboratory, 44 Lincolns Inn Fields, Holborn, London, WC2A 3LY

[5] Orthogon Therapeutics, 960 Turnpike Street, Unit 10, Canton, MA 02021, USA

[6] Sabin Vaccine Institute and Texas Children's Hospital Center for Vaccine Development, 1102 Bates Avenue, Houston, TX 77030, USA

[7] Division of Biological and Environmental Sciences and Engineering, CBRC, King Abdullah University of Science and Technology, Thuwal 23955-6900, Kingdom of Saudi Arabia

[8]Current address: The Gurdon Institute, University of Cambridge, Tennis Court Road, Cambridge, CB2 1QN

*Corresponding author

[†]Authors contributed equally to this work.

Abstract

Scaffold proteins play important roles in regulating signalling network fidelity, the absence of which is often the basis for diseases such as cancer. In the present work, we show that the prototypical scaffold protein Shc is phosphorylated by the extracellular signal-regulated kinase, Erk. In addition, Shc threonine phosphorylation is specifically up-regulated in two selected triple-negative breast cancer (TNBC) cell lines. To explore how Erk-mediated threonine phosphorylation on Shc might play a role in the dysregulation of signalling events, we investigated how Shc affects pathways downstream of EGF receptor. Using an *in vitro* model and biophysical analysis, we show that Shc threonine phosphorylation is responsible for elevated Akt and Erk signalling, potentially through the recruitment of the 14-3-3 ζ and Pin-1 proteins.

Introduction

Scaffold proteins play an important role in propagation of signals from cell surface receptors. Bringing signalling proteins into proximity on a common structure provides increased opportunity for regulation of downstream response through signal specification and amplification. Initiation of signal transduction from receptor tyrosine kinases (RTKs) is dominated by tyrosine phosphorylation, however this is often superseded by serine/threonine kinase up-regulation. Juxtaposing of tyrosine and serine/threonine cognate binding sites on a scaffold protein provides the opportunity for fine-tuning of RTK signal transduction through modulating protein-protein interactions (Deribe et. al., 2010; Johnson und Lewis, 2001; Seet et. al., 2006).

The prototypical scaffold protein ShcA (henceforth Shc) has been extensively studied in regard to its ability to recruit proteins dynamically in RTK-mediated signalling. It plays a complex role as a hub for binding of numerous signalling proteins. Despite having no intrinsic enzyme activity, Shc is involved in signal transduction associated with poor prognosis in breast cancer patients (Ursini-Siegel & Muller, 2008). The *ShcA* gene encodes three isoforms of 46, 52 and 66 kDa (p46, p52 and p66 respectively) which all possess an N-terminal PTB domain and a C-terminal SH2 domain which sequentially sandwich a CH1 domain. Shc binds through its phosphotyrosine binding (PTB) domain to tyrosyl phosphates on activated RTKs and undergoes a conformational change which exposes its SH2 domain (George et. al., 2008). Within the sequence of Shc are a number of tyrosine, serine and threonine phosphorylation sites which enable Shc to recruit a large, multi-functional array of proteins which appear to be temporally controlled subsequent to RTK activation (Zheng et. al., 2013). Shc therefore forms a dynamic hub for protein recruitment.

It has been demonstrated that under non-stimulated conditions Shc (p52Shc) binds directly to the proline-directed serine/threonine kinase, Erk (extracellular signal-regulated kinase, aka. mitogen-activated protein kinase (MAPK)) (Suen et. al., 2013). In so doing Erk is restricted from engaging in MAPK signalling. Erk is released from Shc and becomes up-regulated in response to RTK-activated MAPK signalling. On activation Erk phosphorylates a wide range of downstream effector protein substrates (Arur et. al., 2009; Carlson et. al., 2011), including several scaffold proteins, e.g. Grb2-associated binding protein 1 (Gab1) (Gu und Neel, 2003; Lehr et. al., 2004; Roshan et. al., 1999; Yu et. al., 2002), fibroblast growth factor receptor substrate 2 alpha (Frs2α) (Lax et. al., 2002; Wu et. al., 2003) and insulin

receptor substrate 1 (IRS1) (Arur et. al.., 2009; De Fea et. al., 1997). While Shc has recently been established to be a substrate for Erk, the significance of these phosphorylation events has not been investigated (Zheng et. al., 2013). Erk-mediated phosphorylation of Shc could regulate its ligand binding capability allowing modulation of downstream signalling.

Serine/threonine and tyrosine phosphorylation are considered to be inversely correlated events, for example phosphorylation on serine/threonine residues of a scaffold protein reduces the level of tyrosine phosphorylation. Since phosphorylated tyrosine residues are required to propagate downstream signalling from a RTK, reduction in signalling through subsequent serine/threonine phosphorylation results in a negative feedback mechanism for pathway control (Lax et. al., 2002; Yu et. al., 2002). Interestingly, a positive feedback role for serine/threonine phosphorylation on scaffold proteins has also been shown. For example, Erk phosphorylation of Gab1 enhances the recruitment of the p85 subunit of phosphoinositide 3-kinase (PI3K) to Gab1, resulting in an increase in PI3K and Erk signalling (Yu et. al., 2001).

Here we show that three threonine residues on Shc are selectively phosphorylated by Erk *in vitro* and in breast cancer cell lines post-EGF stimulation. Phosphorylation of these residues leads to elevated Erk and Akt phosphorylation post-EGF stimulation. We demonstrate how phosphorylation on one of these residues appears in two selected triple-negative breast cancer cell lines and investigate the structural implications of these phosphorylation events. We identify two proteins whose phosphothreonine-dependent association with Shc provides evidence for additional downstream signal mediation.

Results

Three threonine residues on Shc are substrates for Erk

Three threonine residues on Shc (T214, T276 and T407) are contained within the Erk consensus substrate sequence (S/T-P). Incubation of purified Shc with active Erk2 in the presence of ATP and $MgCl_2$ revealed that Shc is threonine phosphorylated on the putative Erk substrate sites (Figure 1A). Since the commercially available pan-anti-T-P antibody cannot distinguish between the three substrate sites for Erk on Shc, we analysed Erk-phosphorylated, trypsin-digested Shc by mass spectrometry. This showed that three T-P motifs on p52Shc were phosphorylated after incubation with Erk (Supplemental Figure 1). Of the three sites only T214 has previously been shown to be a substrate for Erk (Zheng et. al., 2013). Phosphorylation of T276 on p66Shc by an unknown kinase (Khanday et. al., 2006; Rajendran et. al., 2010) has previously been reported. T214 and T276 are found in the CH1 domain, whilst T407 is in the SH2 domain (Figure 1B). Both T214 and T407 are highly conserved across various species, whereas T276 is less so (Figure 1C).

Since phosphorylation of Shc has previously been shown to exert regulatory control of ligand binding (George et. al., 2008), we investigated whether the phosphorylation of threonine residues affected the ability of Shc to bind to a RTK. We expressed and purified a triple mutant form of Shc in which the three threonine residues were replaced by the phosphorylation charge mimetic of threonine; glutamate (T214/276/407E or ^{TE}Shc) and measured its binding to a known Shc-binding peptide corresponding to the TrkA receptor. The mutation of the threonine residues to glutamate mimics the triple phosphorylated state of Shc. Isothermal titration calorimetric (ITC) data show that the phosphorylation state of

the threonine residues has no effect on recruitment to the receptor demonstrated by the comparable dissociation constants for the binding wild type, ^{WT}Shc, or ^{TE}Shc to the RTK-derived peptide ($K_d \sim 54$nM and 38nM, respectively; Figure 1D).

We previously reported a gating mechanism driven by tyrosine phosphorylation on Shc, whereby the SH2 domain is only available for ligand-binding when the CH1 domain is phosphorylated on its tyrosine residues (George et. al., 2008). It has also been proposed that phosphorylation on Y317 introduces rigidity to the protein and limits the dynamic motions of the PTB and SH2 domains in molecular dynamics simulation studies (Suenaga et. al., 2009, 2004). Hence, there is a precedent for regulation imposed by inter-domain interactions. We therefore explored the possibility that threonine phosphorylation induces a conformational change in Shc. The structural model of the full length Shc protein suggests that T214 and T276 reside on helices (PDB 1WCP)(Suenaga et. al., 2004). We therefore employed circular dichroism spectroscopy (CD) to investigate the effect of threonine phosphorylation on the secondary structure of Shc. We compared the CD signals from the full length unphosphorylated and threonine-phosphorylated Shc. As expected the CD signal is commensurate with the full length Shc protein (ShcFL) containing α-helical, β-strand and disordered structure (Supplemental Table 1). However, no significant changes in the structural composition between unphosphorylated and threonine-phosphorylated forms were observed as shown by the overlapping signals from the wild type and mutant Shc proteins (Figure 1E). A further lack of impact on the protein structure was reflected in the thermostability of Shc which was unaffected by threonine phosphorylation Shc (Figure 1F). Finally, the similar pattern of protease digestion observed for the ^{WT}Shc and ^{TE}Shc proteins

(Fontana et. al., 2004) confirmed that no structural variation was imparted by threonine phosphorylation (Supplemental Figure 2).

Phosphorylation of T214 is prevalent in triple-negative breast cancer cells

To investigate the potential pathological relevance of the threonine phosphorylation events we screened for the presence of phosphorylation on T214 (pT214) in a number of transformed/cancer cell lines with a specific antibody against pT214 (efficiency of antibody shown in Supplemental Figure 3). We initially focused on breast cancer due to the previously reported critical role of Shc in this disease (Ursini-Siegel & Muller, 2008) (Figure 2 and Supplemental Figure 4). Non-transformed MCF10A cells (Soule et. al., 1990) were used for comparison with the selected cancer cell lines (Figure 2C). Cells were stimulated with EGF for between 2 and 30 minutes to investigate the temporal pattern of Shc threonine phosphorylation. Cells were also separately pre-incubated with the MAPK/Erk kinase, Mek, inhibitor U0126 to abolish Erk activity (Mek is upstream of, and responsible for phosphorylation and activation of Erk), in order to confirm that the phosphorylation event is mediated by Erk. We first immunoprecipitated total Shc and then probed for pT214. Although all cell lines exhibited Erk activity upon EGF stimulation, only the triple negative cell lines MDA-MB-468 and MDA-MB-231 exhibited a significant level of phosphorylation on T214 (Figures 2A and 2B). None of the other cell lines tested showed evidence of phosphorylated T214, (i.e. non-transformed MCF10A cells (Figure 2C) and other non-triple negative cell lines; MCF7 (Figure 2D), MDA-MB361, A431, HEK293T (Supplemental Figure 4)). Two of the known binding partners for Shc in EGF signalling, epidermal growth factor receptor, EGFR, and growth factor receptor protein-binding protein 2, Grb2, were probed as

controls for Shc function (Figure 2A-D and Supplemental Figure 4). To confirm that Shc is threonine phosphorylated in the triple-negative cell lines, we immunoprecipitated Shc using the pT214 antibody and then probed for Shc (Figures 2E and 2F). In agreement with the previous immunoprecipitation experiments, Shc is phosphorylated on T214 in both MDA-MB-468 and MDA-MB-231 cells.

It has been reported that serine/threonine phosphorylation affects tyrosine phosphorylation in scaffold proteins, so we examined the phosphorylation levels on the three known Shc tyrosine sites, 239, 240 and 317 in response to threonine phosphorylation. If Shc threonine phosphorylation affects the concomitant tyrosine phosphorylation level, we should observe a consistent change in Shc tyrosine phosphorylation when the cells are treated with the Mek inhibitor. As expected treatment with U0126 abrogated phosphorylation of T214, however the effect on the tyrosine residues across the breast cancer cell lines was inconsistent and showed no correlation with the threonine phosphorylation observed in triple negative cells (Figure 2A-D). In other words abrogation of threonine phosphorylation did not have a uniform effect on tyrosine phosphorylation.

Shc threonine phosphorylation up-regulates Erk and Akt phosphorylation

Given that Shc is threonine phosphorylated in the metastatic cell lines MDA-MB-468 and MDA-MB-231 (Jin et. al., 2012; Kang et. al., 2003; Kathryn et. al., 2012) but not the non-transformed MCF10A cells (Debnath et. al., 2003), we hypothesise that Shc threonine phosphorylation contributes towards the cellular signalling that is responsible for the oncogenic properties reflected in these cell lines. To test this hypothesis we mutated all

three threonine residues (T214/276/407) either to alanine (^{TA}Shc: phosphorylation-deficient mutant) or glutamate residues (^{TE}Shc: phosphorylation-mimetic mutant) and stably over-expressed these constructs in HEK293T cells. Both EGFR and Shc regulate tumorigenic signalling via the Erk and Akt pathways (Herbst, 2004; Manning & Cantley, 2007; Roberts & Der, 2007; Ursini-Siegel et. al., 2012; Wills & Jones, 2012), therefore we evaluated the phosphorylation levels of Erk and Akt over a time course after EGF stimulation in the presence of the mutant forms of Shc. We found that in cells over-expressing ^{TE}Shc consistently higher levels of Erk phosphorylation across the time course were observed compared to ^{WT}Shc and ^{TA}Shc over-expressing cells (Figure 3A and 3B). This suggests that the threonine phosphorylation amplifies the level of Erk phosphorylation post-EGF stimulation. Shc therefore functions with Erk in a positive feedback loop in which Erk up-regulation post growth factor stimulation enhances the potency of its signal through phosphorylation of Shc; as has been reported for other scaffold proteins including Gab and Frs2 (Lax et. al., 2002; Wu et. al., 2003). The level of Akt phosphorylation was also seen to be affected by the presence of threonine phosphorylation. We observed a pronounced increase in Akt phosphorylation from 2 minutes up until 30 minutes post-EGF stimulation in cells overexpressing ^{TE}Shc compared with cells overexpressing ^{WT}Shc and ^{TA}Shc (Figure 3A, 3C and Supplemental Figure 6). Therefore a cross-talk mechanism exists between the Erk and Akt signalling pathways whereby Erk-mediated phosphorylation of Shc upregulates Akt activity. This is an unexpected result because previous reports suggested that expression of the T214A phosphorylation-deficient Shc mutant led to only a moderate increase in cell numbers when compared with wild-type Shc (Zheng et. al., 2013), which might be indicative of downregulation of proliferative Akt signalling when Shc is threonine phosphorylated.

Furthermore, ^{TE}Shc is able to 1) elicit Akt phosphorylation even in the absence of EGF stimulation and 2) sustain Akt phosphorylation for longer than Erk phosphorylation. Both of these observations suggest the primary role of Shc threonine phosphorylation is to modulate the Akt pathway. The relatively mild positive feed-back loop that Shc and Erk engage in could be a by-product of the excess Akt activation that led to a delay in Erk dephosphorylation, possibly due to limiting common components (Mendoza et al., 2011). The fact that ^{TE}Shc upregulates Akt phosphorylation without the activation of Erk indicates that ^{TE}Shc is able to directly recruit downstream factors that lead to Akt activation. We note that both Erk and Akt phosphorylation levels are similar between ^{WT}Shc and ^{TA}Shc cells. This is consistent with the observation that there is no or a very low level of Shc threonine phosphorylation in HEK293T cells (Supplemental figure 4C).

Protein recruitment is dependent on threonine phosphorylation of Shc

A large array of proteins bind to phosphorylated threonines or serines (Seet et. al., 2006; Yaffe & Elia, 2001). We performed a literature search to identify proteins that would be potential ligands for Shc after threonine phosphorylation. We selected three isoforms of the scaffold protein 14-3-3 (Fu et. al., 2000), the E3 ubiquitinase, neural precursor cell expressed developmentally down-regulated protein 4, Nedd4 (Ingham et. al., 2004) and peptidyl-prolyl cis-trans isomerase NIMA-interacting 1, Pin1 (Lu et. al., 2007; Pinton et. al., 2007; Zheng et. al., 2013) as possible candidates. 14-3-3 proteins are known to binding to phosphorylated threonines and serines, while both Nedd4 and Pin1 contain WW domains that recognize either proline-rich or pThr/Ser motifs. These proteins were over-expressed, isolated and immobilized on agarose beads through fusion tags, and used as bait for pull-down

experiments. Cell lysates from the MDA-MB-468 cell line were used for 'fishing' since Shc is threonine phosphorylated within 5 minutes of EGF stimulation in these cells (Figure 2A). Cells were starved overnight and then stimulated with EGF for 5 minutes. Erk activity was inhibited by the use of the Mek inhibitor U0126 to abolish Erk–mediated Shc threonine phosphorylation.

All proteins tested were able to pull-down Shc (Figure 4). Nedd4 binds to Shc constitutively, which suggests that the interaction is driven by the proline-rich motifs within the CH1 domain of Shc rather than phosphorylation (Figure 4A). All three 14-3-3 isoforms could bind to threonine phosphorylated Shc in an EGF stimulation-dependent manner although they were differentially affected by Erk activity (Figure 4B and 4C). When Erk activity is inhibited the ζ isoform interaction with Shc is reduced, whereas the binding between Shc and 14-3-3τ and 14-3-3ε remained unchanged. 14-3-3ζ has been previously reported to up-regulate PI3K signalling when recruited to Shc (Ursini-Siegel et. al., 2012), it is therefore likely that threonine-phosphorylated Shc augments Akt phosphorylation by interacting with 14-3-3ζ. Finally, Pin1 interacts with Shc when cells are stimulated with EGF and the binding is abolished when Erk activity is inhibited. This is consistent with the fact that Pin1 binding and activity are pT/S-dependent. A C113A mutation in Pin1, which has been identified as affecting the isomerase activity without affecting binding to pT (Ranganathan et. al., 1997), did not affect its binding to Shc (Figure 4D).

For proteins whose binding to Shc rely on Erk activation and hence indicating a Shc-threonine-dependent mechanism, we further tested for their ability to interact with the Shc

phospho-mimic (^{TE}Shc) in HEK293T cells. Both Pin1 and 14-3-3 ζ pulldown with ^{TE}Shc at a higher level than ^{TA}Shc (Supplemental Figure 7 and 8). Therefore, we surmise that Pin1 and 14-3-3 ζ bind to threonine phosphorylated Shc.

We used microscale thermophoresis, MST, to measure the binding of 14-3-3ζ (Supplementary Figure 5A-C) and Pin1 (Supplementary Figure 5D and E) to phosphopeptides containing the sequences including and proximal to pT214, pT276 and pT407. Fluorescently-labelled 14-3-3ζ or Pin1 were incubated with the individual Shc phosphothreonine peptides. Although none of the three Shc threonine phosphorylation sites include the canonical binding sequence for 14-3-3ζ(Fu et. al., 2000), we detected binding between 14-3-3ζ and both pT276 (K_d=9.8μM) and pT407 (K_d=2.1μM). To confirm 14-3-3ζ is able to interact with pT407 within the context of a folded protein domain, we purified Shc SH2 domain with a phospho-mimic mutation (T407E; herein referred to as SH2TE) and measured the binding. In agreement with the peptide data, 14-3-3ζ binds to Shc SH2TE with a similar affinity as with pT407 (K_d=1.9μM; Supplementary Figure 5F). Unlike 14-3-3ζ, Pin1 appears to show a preference for the pT407 (K_d=39μM) over the pT214 (K_d=575μM) peptides, suggesting that the sequences flanking the pT contribute to the binding affinity for the two proteins.

Discussion

In this investigation we demonstrate that the role of Shc in signal transduction is greater than just a 'passive' scaffold. Through phosphorylation by Erk and binding to selective downstream effectors Shc can modulate signalling response. Upon activation of EGFR, Erk

phosphorylates Shc on three residues resulting in up-regulation of a positive feedback loop in Erk-signalling and crosstalk between the Erk and Akt pathways (Figure 5). Up-regulation of proliferative signalling events relate to the finding that a significant level of phosphorylation of T214 in two triple-negative breast cancer cell lines, MDA-MB-468 and MDA-MB-231, but not in the non-transformed MCF10A cell line. It is interesting to note that while Erk can be phosphorylated in all of the tested cell lines, only the two TNBC cell lines exhibit detectable Erk-dependent Shc T214 phosphorylation. One reason could be that these cell lines may engage slightly different protein components downstream of EGF receptor activation. For example, the serine/threonine phosphatase PP2A, which has been shown to interact with Shc, is downregulated in breast cancer cells (Seshacharyulu et al., 2013). It is possible that the activity of PP2A is higher in certain cell lines and therefore dephosphorylation of the pathways occur more quickly and Shc T214 phosphorylation is thus too transient to be captured in our experimental setup. Indeed, it has been shown that in MDA-MB-231, but not MCF7, cells that PP2A is inactivated by the over-expression of its inhibitor CIP2A and that tamoxifen treatment leads to the activation of PP2A and downregulation of Akt phosphorylation (Liu et. al.., 2014).

Threonine phosphorylation does not appear to induce any structural perturbation (as has been observed on tyrosine phosphorylation (George et. al., 2008)) even though two of the residues are in the intrinsically disordered CH1 domain. However, the formation of these new phospho-motifs alter protein recruitment. We identified two proteins, Pin1 and 14-3-3ζ whose binding to Shc is pT-dependent. Previous reports show that 14-3-3ζ binding to the SH2 domain of Shc is mediated by the phosphorylation of 14-3-3ζ on tyrosine 179 which

leads to upregulation of PI3K and subsequently Akt signalling (Barry et. al., 2009; Ursini-Siegel et. al., 2012). Our data suggest an additional mechanism for this interaction whereby 14-3-3ζ binds to threonine phosphorylated Shc. Recruitment of 14-3-3ζ to Shc has been shown to increase PI3K signalling (Ursini-Siegel et. al., 2012). Given that PI3K is an upstream activator of Akt, it seems likely that this interaction is at least partially responsible for the elevated pAkt level seen in ^{TE}Shc cells (Vanhaesebroeck et. al., 2012).

Pin 1 isomerizes only phospho-serine/threonine-proline motifs and plays a role as a post-phosphorylation regulator of protein function and hence is implicated in cancer. Pin1 has previously been shown to recruit p66Shc to the mitochondria in a PKC-dependent manner, which is a process that leads to apoptosis (Pinton et. al., 2007). Here we show that p52Shc can also bind to Pin1, albeit through different phosphothreonine residues. Some peptide prolyl cis-trans isomerases (PPIases), such as Pin1 specifically catalyse isomerisation of prolines preceded by pS/pT. PPIases catalyse the conversion of the cis-trans conformation of proline which can potentially switch local conformations from one to another (Lu & Zhou, 2007) and adjust protein-recruitment profiles. In addition, because some phosphatases, such as PP2A, only act on certain phospho-isoforms, proline-isomerization can also alter the rate of phosphorylation/dephosphorylation (Lu & Zhou, 2007; Zhou et. al., 2000). We have previously identified another PPIase, cyclophilin A (CypA) as a direct binding partner for Shc (George et. al., 2009). Given that the CH1 domain is proline-rich, there is a strong possibility that proline isomerization provides an additional mode of regulation.

Finally, in light of the finding that the level of Shc threonine phosphorylation is higher in two TNBC cell lines, the Shc threonine phosphorylation sites could potentially serve as markers for a subtype of TNBC. The two TNBC cell lines in which we found pT214 to be significantly phosphorylated exhibit over-expression of EGFR and mutant KRAS expression (Kathryn et. al., 2012; Kenny et. al., 2007). While TNBC describes a collection of disease states with highly variable genotypes, some can be classified in sub-groups by other markers, such as their EGFR expression status (Ferraro et. al., 2013; Park et. al., 2014). If this threonine phosphorylation effect is reproduced in other TNBC this could provide a viable basis for biomarker development.

Materials and Methods

Reagents

Antibodies for pErk (4695), Erk (4377), pT308Akt (4056), Akt (4691), pT-P (9391), pY239/240Shc (2434), EGFR (2646), GST (2625), 14-3-3 (8312) were obtained from Cell Signaling Technology; pY317 (sc-23765R), HA-tag (sc-805), GFP (sc-9996) were obtained from Santa Cruz; Shc (MAB0807) and Strep-tag (PAB-16601) was obtained from Abnova. The custom antibody for pT214 Shc was generated against peptide NPPKLVpTPHDRMAG by Genscript. Lysis buffer: 50mM HEPES, pH7.5, 50mM NaCl, 1mM EGTA, 10% (w/v) Glycerol, 1mM Sodium orthovanadate, 10mM Sodium fluoride, 0.1% NP-40, 1x protease and phosphoSTOP inhibitors (Roche). Shc phosphothreonine peptides (pT214: CNPPKLVpTPHDRMAG; pT276: CARPTAPNAQpTPSHL; pT407: CDFLVRESTTpTPGQ were purchased from Genescript.

Mammalian cell culture

HEK293T, MCF7, MDA-MB-468, MDA-MB-231, A431, PC12 cells were maintained as described previously (Suen et. al., 2013); MDA-MB-361 cells was grown in DMEM/F12 supplemented with 10% FBS. MCF10A cells were grown as previously described (Debnath et. al., 2003). Transfection HEK293T cells and generation stable cell lines were described previously(Suen et. al., 2013).

Molecular biology

^{TA}Shc and ^{TE}Shc mutants were generated by site-mutagenesis. The following constructs were obtained from Addgene: GST-tagged 14-3-3 ε (13279), GST-tagged 14-3-3 τ (13281), and 14-3-3 ζ (mouse; 1942), GST-Pin1 (19027), HA-Nedd4 (27002), His-tagged Pin1 (40773). A mutation of P112A was made in mouse 14-3-3 zeta to match the human sequence and was then subcloned into the pEGFP-N vector. C113A mutation was made in GST-Pin1 by site-directed mutagenesis.

***In vitro* Erk2 phosphorylation of full length Shc (ShcFL)**

50 µl of 10µM purified ShcFL proteins in PBS were incubated with 1µl of active Erk2 (NEB, P6080) in the presence of 5mM buffered ATP and 10mM $MgCl_2$ overnight.

Protein expression and purification

To express and purify GFP-14-3-3 and HA-Nedd4, HEK293T cells were transfected with 20 ug of GFP-N-14-3-3 ζ plasmids on a 10cm-dish. 2x 10cm-dishes were used per pull-down experiment. Cells were harvested and lysed in 1ml of lysis buffer 48hrs after transfection.

Cleared lysates was incubated with 50ul GFP-trap beads overnight. Beads were washed with 1ml lysis buffer 5-10 times. Recombinant his-tagged Shc was expressed and purified as described previously (George et. al., 2008). Phosphorylated his-tagged Shc was purified with the additional step of IMAC to remove active Erk2. GST-tagged proteins and His-tagged Pin1 were expressed in Rosetta 2. Bacterial culture was inoculated with overnight culture in 1:1000 ratio and grown to OD_{600} 0.8 at 37°C. The temperature was then reduced to 20°C and induced with 0.1mM IPTG for overnight. His-tagged Pin1 was purified first by affinity chromatography, followed by a size exclusion step to exchange into final buffers. GST-tagged proteins were immobilized on glutathione-sepharose resins and washed extensively in 50mM Tris pH8.0, 150mM NaCl and 0.1% Triton-X100. GST-proteins were then stored at -20 in 50% glycerol until required.

Pull-down experiments

Purified proteins immobilized on beads were incubated with MDA-MB-468 cell lysates overnight. 500ug of lysates were used per pull-down. Samples were then washed in 3x1ml lysis buffer and then boiled in Laemmli buffer before analysed by SDS-PAGE and western blotting.

Immunoprecipitation

Cells were lysed in lysis buffer (typically 1ml of lysis buffer was used on a 10cm-dish) and cleared by centrifugation. One milligram of lysate was used per IP experiment. IP antibody was added to the lysate and incubated for overnight. 25 µl of Protein A/G slurry was added

to the lysate for 2 h. The immunoprecipitants were washed three times with lysis buffer and boiled with 2× sample buffer for 5 min to elute.

Isothermal titration calorimetry, ITC, experiment

Experiments were performed using the VP instrument (GE, Northampton, MA) at 13 °C in 20 mM HEPES, pH 7.4, 50 mM NaCl, 3 mM EDTA and 5 mM βME. ITC binding data were corrected for heats of dilution. ORIGIN7 software was used for data analysis using the single site model.

Microscale thermophoresis, MST, experiment

Protein was labeled using the Nanotemper labeling kit. Briefly, ShcPTB was diluted to 20μM in labeling buffer to the final volume of 100μl. 60μM of dye NT-647 was added to the diluted protein and incubated for 2-4hrs at room temperature. ShcPTB was then separated from the free dye using a G25-sephadex column in PBS. Labeling efficiency was typically between 50%-100%. To test binding between ShcPTB and ligands, a 1:2 dilution series of each ligand was prepared with a final volume of 10μl. Experiments were carried out at 25°C.

Circular dichroism, CD, spectroscopy

All CD spectra were recorded at room temperature a Jasco J-810 spectropolarimeter in PBS. Data was collected at 0.2nm intervals in triplicates.

Differential scanning fluorescence analysis

5μM ShcFL proteins were incubated with 1:2000 SYPRO Orange dye dilution (Invitrogen) to a final volume of 20μl at 4°C for 20 minutes. Melting assay was performed on Roche LightCycler 480 instrument by applying ROX filter for the fluorescence emission (610 nm) and FAM filter for the fluorescence excitation (492 nm). Fluorescence was monitored between 20°C and 95°C. Fluorescence signals from the fully folded and unfolded states were plotted as 0% (fully folded) to 100% (fully unfolded).

Limited proteolysis

100ng of ShcFL proteins were incubated with 0.5ng of chymotrypsin in PBS at 37°C for each time point. Digestion process was terminated by the addition of 2X loading sample buffer and boiling for 5min.

Figure Legends

Figure 1: Identification of Erk phosphorylation sites on p52Shc. (A) Phosphorylation of Shc on Erk substrate motifs (T-P) 10μM of 50μl purified Shc protein was incubated with 1μl of active Erk2 in the presence or absence of ATP and $MgCl_2$ for the indicated time periods. Phosphorylation of T-P motifs on Shc was analyzed by western blotting using an antibody specific to pT-P motifs. (B) Location of the threonine residues on Shc phosphorylated by Erk. Three threonine residues on Shc are phosphorylated by Erk: T214 and T276 are in the CH1 domain; T407 is in the SH2 domain. (C) Sequence alignment of ShcA from various species show that T214, T276 and T407 are conserved. Hs: Homo sapiens; Mm: Mus musculus; Rn: Rattus norvegicus; Gg: Gallus gallus; Xl: Xenopus laevis; Ce: Caenorhabditis elegans. (D) ITC measurement of intact ^{WT}Shc and ^{TE}Shc binding to TrkA phosphopeptide. Twenty 10μl injections of tyrosyl phosphorylated TrkA peptide (100μM) were titrated into wild type full length ^{WT}Shc or glutamine triple mutant ^{TE}Shc (10μM) at 13^{o}C. Top panel: baseline-corrected power versus time plot for the titration. Bottom panel: the integrated heats and the molar ratio of TrkA binding to ShcFL. The data were corrected for the heats of dilution of TrkA and fit to a one-site binding model. Left: ^{WT}ShcFL; Right: ^{TE}ShcFL. Titrations were fitted into a one-site model. K_D for ^{WT}Shc and ^{TE}Shc are 53nM±435nM and 38nM±427nM, respectively. (E) CD spectral analysis of ShcFL proteins. The average of three scans at 0.5nm intervals for each sample is plotted. Experiments were carried out at room temperature in PBS. Grey solid line: 5μM unphosphorylated Shc; Black dashed line: 5μM threonine phosphorylated Shc. Data was subtracted from the buffer signal and plotted on Excel. (F) DSF analysis of the thermostability of ShcFL proteins. 5μM of unphosphorylated ShcFL and threonine phosphorylated ShcFL in PBS were incubated with 1x Sypro orange dye and heated from

room temperature to 95°C. Unfolding of proteins was monitored by increase in fluorescence and is plotted as proportion unfolded. Grey solid line: 5μM unphosphorylated Shc; Black dashed line: 5μM threonine phosphorylated Shc.

Figure 2: Phosphorylation of T214 in endogenous Shc in mammalian cell lines. Cells were starved overnight and then stimulated with 20ng/ml EGF for the indicated time periods. The Mek inhibitor U0126 was applied at 10μM for 45 minutes prior to EGF stimulation in '5+U' samples. (A) – (D) Shc was immunoprecipitated from 1mg of lysates. Immunoprecipitants (IP) were probed for pT214 (arrowheads; * denotes non-specific IgG heavy-chain bands) and pY239/240 levels of Shc, the presence of EGFR and Grb2. Whole cell lysates (w.c.l.) of the same samples were also analyzed for pErk level and pY317 of Shc. (A) MDA-MB-468 (B) MDA-MB-231 (C) MCF10A (D) MCF7. (E) – (F) Anti-pT214 antibody was used to immunoprecipitate Shc from 1mg of lysates. Immunoprecipitants (IP) were probed total Shc. (E) MDA-MB-468 (F) MDA-MB-231.

Figure 3: Shc threonine phospho-mimic mutant leads to elevated pAkt and pErk levels. (A) HEK293T cells stably overexpressing either empty vector, strep-tagged ^{WT}Shc, ^{TA}Shc or ^{TE}Shc were starved overnight and then stimulated with 20ng/ml EGF for the indicated time periods. 25μg of total cell lysates were analyzed by western blotting for the phosphorylation states of Akt T308 (upper panels) and Erk (middle panels). Equal expression of the Shc constructs were confirmed by blotting for strep-tag (bottom panel). (B) Phospho-Erk response is normalized against loading and fold-change is expressed as proportion of response from ^{TE}Shc at 5min time-point. (C)Phospho-Akt (308) response is normalized against loading and fold-change is expressed as proportion of response from ^{TE}Shc at 5min

time-point. (B) and (C) Immunoblot bands were quantified by Image J from at least 3 biological repeats. Error bars are standard errors. Blue: ^{WT}Shc ; Red: ^{TA}Shc ; Blue: ^{TE}Shc

Figure 4: Pull-down experiments to identify Shc protein binding partners that are affected by Shc threonine phosphorylation. (A) - (D) Fusion proteins were purified and immobilized on agarose beads and incubated with MDA-MB-468 lysates overnight. Beads were washed with lysis buffer and the samples were analyzed by western blotting for the presence of Shc. (A) HA-tagged Nedd4 (B) GFP-14-3-3 ζ (C) GST-14-3-3 τ and GST 14-3-3 ε (D) GST-Pin1 WT or C113A.

Figure 5 Schematic summary of the mutual regulation between Shc and Erk. In the absence of extracellular stimulation to EGFR (green), Shc (blue) and Erk (magenta) form a complex in the cytoplasm which inhibits up-regulation of Erk by Mek (Suen et al 2013). Upon EGF stimulation, Shc binds to the activated EGFR, which triggers a conformational change in Shc and leads to Erk dissociation from the complex. Shc is phosphorylated by the receptor (red arrows) on its tyrosine residues (green circles/yellow outline), which recruits the Grb2 (red)-Sos (olive green) complex to the membrance. This activates Ras, which initiates the activation of the Erk cascade (purple arrow). Activated Erk phosphorylates Shc (blue arrow) on threonine residues (cyan circles/blue outline), which further elevates the Erk phosphorylation and activates Akt, possibly through the recruitment of 14-3-3 zeta-p85 complex (including p85 subunit of PI3K (brown)).

Supplemental Figures:

Figure 1: Mass Spectrometry analysis of phosphorylation status of Shc TP motifs. 50µl of purified Shc at 100µM and incubated with 10µl of active Erk2 in the presence of $MgCl_2$ and ATP for 16h at 20 ^{o}C. The mass spectra for (A) T214 (B) T276 and (C) T417. Mass spectrometry measurements and analysis were performed by the MDACC core. (D) Sequences of Erk-mediated phosphorylation on Shc.

Figure 2: Limited proteolysis analysis of ShcFL proteins. 100ng of ^{WT}Shc or ^{TE}Shc was incubated with 1ng of chymotrypsin at 37^{o}C for various periods of time as indicated. Samples were analyzed by SDS-PAGE, followed by silver staining.

Figure 3: Specificity test for anti-pT214 antibody. Purified recombinant Shc was phosphorylated by active Erk2. A western blot signal is only present when Shc was phosphorylated by Erk2. This confirms that the anti-pT214 antibody is specific for phosphorylated Shc.

Figure 4: Phosphorylation of T214 in endogenous Shc in mammalian cell lines. Cells were starved overnight and then stimulated with 20ng/ml EGF for the indicated time periods. The Mek inhibitor U0126 was applied at 10µM for 45 minutes prior to EGF stimulation in '5+U' samples. Shc was immunoprecipitated from 1mg of lysates. Immunoprecipitants (IP) were probed for pT214 and pY239/240 levels of Shc, the presence

of EGFR and Grb2. Whole cell lysates (w.c.l.) of the same samples were also analyzed for pErk level and pY317 of Shc. (A) MDA-MB-361 (B) A431 (C) HEK293T. (D) – (E) Anti-pT214 antibody was used to immunoprecipitate threonine phosphorylated Shc from lysates. Immunoprecipitants (IP) were probed total Shc. (D) MCF10A (E) MCF-7.

Figure 5: **Biophysical analysis of 14-3-3 ζ and Pin1 binding to Shc phosphopeptides.** Purified recombinant 14-3-3 ζ and Pin1 were labeled with the fluorescent NT-647 dye. The labeled proteins were incubated with the indicated ligands and fluorescence was monitored. The binding curves were fitted by the law of mass action. (A) 14-3-3 ζ with pT276 (B) 14-3-3 ζ with pT407 (C) 14-3-3 ζ with ShcSH2^{TE} (D) Pin1 with pT214 (E) Pin1 with pT407 (F) Table with fitted K_D.

Figure 6: **Shc threonine phospho-mimic mutant leads to elevated pAkt 473.** HEK293T cells stably overexpressing either strep-tagged ^{WT}Shc, ^{TA}Shc or ^{TE}Shc were starved overnight and then stimulated with 20ng/ml EGF for 5 min. Total cell lysates were analyzed by western blotting for the phosphorylation states of Akt T473.

Figure 7: **Pin1 interacts with Shc^{TE} mutant in HEK293T cells.** Purified recombinant Pin1 WT protein fused with GST was incubated with lysates from HEK293T cells overexpressing either strep-tagged ^{WT}Shc, ^{TA}Shc or ^{TE}Shc. Cells were starved overnight and stimulated with 20ng/ml of EGF for 5min. To assess interaction between Shc mutants and Pin1, samples were analysed by western blotting for the presence of strep-tagged Shc.

Figure 8: **14-3-3 ζ interacts with ShcTE mutant in HEK293T cells.** GFP or GFP-tagged 14-3-3 ζ was transiently expressed in HEK293T cells stably overexpressing either strep-tagged ^{WT}Shc, ^{TA}Shc or ^{TE}Shc. Cells were starved overnight and stimulated with 20ng/ml of EGF for 5min. To assess interaction between Shc mutants and 14-3-3 ζ, samples were analysed by western blotting for the presence of strep-tagged Shc.

Table 1: Composition of Shc proteins secondary structures derived from CD spectra. Analysis of the CD signals from ShcFL proteins was analyzed by the CDSSTR software (Fontana et. al., 2004). ShcFL proteins are composed of α-helices, β-strand, turns and disordered regions. Both ^{WT}Shc and ^{TE}Shc have similar compositions.

References

Arur, S., Ohmachi, M., Nayak, S., Hayes, M., Miranda, A., Hay, A., Golden, A., Schedl, T., 2009. Multiple ERK substrates execute single biological processes in Caenorhabditis elegans germ-line development. Proc. Natl. Acad. Sci. U. S. A. 106, 4776–4781. doi:10.1073/pnas.0812285106

Barry, E.F., Felquer, F.A., Powell, J.A., Biggs, L., Stomski, F.C., Urbani, A., Ramshaw, H., Hoffmann, P., Wilce, M.C., Grimbaldeston, M.A., Lopez, A.F., Guthridge, M.A., 2009. 14-3-3:Shc scaffolds integrate phosphoserine and phosphotyrosine signaling to regulate phosphatidylinositol 3-kinase activation and cell survival. J. Biol. Chem. 284, 12080–12090. doi:10.1074/jbc.M807637200

Carlson, S.M., Chouinard, C.R., Labadorf, A., Lam, C.J., Schmelzle, K., Fraenkel, E., White, F.M., 2011. Large-Scale Discovery of ERK2 Substrates Identifies ERK-Mediated Transcriptional Regulation by ETV3. Sci. Signal. 4, rs11-rs11. doi:10.1126/scisignal.2002010

De Fea, K., Roth, R. A, 1997. Modulation of insulin receptor substrate-1 tyrosine phosphorylation and function by mitogen-activated protein kinase. J. Biol. Chem. 272, 31400–6.

Debnath, J., Muthuswamy, S.K., Brugge, J.S., 2003. Morphogenesis and oncogenesis of MCF-10A mammary epithelial acini grown in three-dimensional basement membrane cultures. Methods. doi:10.1016/S1046-2023(03)00032-X

Deribe, Y.L., Pawson, T., Dikic, I., 2010. Post-translational modifications in signal integration. Nat. Struct. Mol. Biol. 17, 666–72. doi:10.1038/nsmb.1842

Ferraro, D. a, Gaborit, N., Maron, R., Cohen-Dvashi, H., Porat, Z., Pareja, F., Lavi, S., Lindzen, M., Ben-Chetrit, N., Sela, M., Yarden, Y., 2013. Inhibition of triple-negative breast cancer models by combinations of antibodies to EGFR. Proc. Natl. Acad. Sci. U. S. A. 110, 1815–20. doi:10.1073/pnas.1220763110

Fontana, A., De Laureto, P.P., Spolaore, B., Frare, E., Picotti, P., Zambonin, M., 2004. Probing protein structure by limited proteolysis, in: Acta Biochimica Polonica. S. 299–321. doi:035001299

Fu, H., Subramanian, R.R., Masters, S.C., 2000. 14-3-3 Proteins: Structure, Function, and Regulation. Annu. Rev. Pharmacol. Toxicol. 40, 617–47. doi:10.1146/annurev.pharmtox.40.1.617

George, R., Chan, H.-L., Ahmed, Z., Suen, K.M., Stevens, C.N., Levitt, J.A., Suhling, K., Timms, J.,

Ladbury, J.E., 2009. A complex of Shc and Ran-GTPase localises to the cell nucleus. Cell. Mol. Life Sci. 66, 711–720. doi:10.1007/s00018-009-8667-8

George, R., Schuller, A.C., Harris, R., Ladbury, J.E., 2008. A Phosphorylation-Dependent Gating Mechanism Controls the SH2 Domain Interactions of the Shc Adaptor Protein. J. Mol. Biol. 377, 740–747. doi:10.1016/j.jmb.2007.12.040

Gu, H., Neel, B.G., 2003. The „Gab“ in signal transduction. Trends Cell Biol. doi:10.1016/S0962-8924(03)00002-3

Herbst, R.S., 2004. Review of epidermal growth factor receptor biology. Int. J. Radiat. Oncol. Biol. Phys. doi:10.1016/j.ijrobp.2003.11.041

Ingham, R.J., Gish, G., Pawson, T., 2004. The Nedd4 family of E3 ubiquitin ligases: functional diversity within a common modular architecture. Oncogene 23, 1972–1984. doi:10.1038/sj.onc.1207436

Jin, W., Chen, B., Li, J., Zhu, H., Huang, M., Gu, S., Wang, Q., Chen, J., Yu, S., Wu, J., Shao, Z., 2012. TIEG1 inhibits breast cancer invasion and metastasis by inhibition of epidermal growth factor receptor (EGFR) transcription and the EGFR signaling pathway. Mol. Cell. Biol. 32, 50–63. doi:10.1128/MCB.06152-11

Johnson, L.N., Lewis, R.J., 2001. Structural basis for control by phosphorylation. Chem. Rev. doi:10.1021/cr000225s

Kang, Y., Siegel, P.M., Shu, W., Drobnjak, M., Kakonen, S.M., Cord??n-Cardo, C., Guise, T.A., Massague, J., 2003. A multigenic program mediating breast cancer metastasis to bone. Cancer Cell 3, 537–549. doi:10.1016/S1535-6108(03)00132-6

Kathryn, J.C., Sireesha V, G., Stanley, L., 2012. Triple Negative Breast Cancer Cell Lines: One Tool in the Search for Better Treatment of Triple Negative Breast Cancer. Breast Dis 32,

35–48. doi:10.3233/BD-2010-0307.Triple

Kenny, P.A., Lee, G.Y., Myers, C.A., Neve, R.M., Semeiks, J.R., Spellman, P.T., Lorenz, K., Lee, E.H., Barcellos-Hoff, M.H., Petersen, O.W., Gray, J.W., Bissell, M.J., 2007. The morphologies of breast cancer cell lines in three-dimensional assays correlate with their profiles of gene expression. Mol. Oncol. 1, 84–96. doi:10.1016/j.molonc.2007.02.004

Khanday, F.A., Yamamori, T., Mattagajasingh, I., Zhang, Z., Bugayenko, A., Naqvi, A., Santhanam, L., Nabi, N., Kasuno, K., Day, B.W., Irani, K., 2006. Rac1 leads to phosphorylation-dependent increase in stability of the p66shc adaptor protein: role in Rac1-induced oxidative stress. Mol. Biol. Cell 17, 122–9. doi:10.1091/mbc.E05-06-0570

Lax, I., Wong, A., Lamothe, B., Lee, A., Frost, A., Hawes, J., Schlessinger, J., 2002. The docking protein FRS2alpha controls a MAP kinase-mediated negative feedback mechanism for signaling by FGF receptors. Mol. Cell 10, 709–719. doi:10.1016/S1097-2765(02)00689-5

Lehr, S., Kotzka, J., Avci, H., Sickmann, A., Meyer, H.E., Herkner, A., Muller-Wieland, D., 2004. Identification of major ERK-related phosphorylation sites in Gab1. Biochemistry 43, 12133–12140. doi:10.1021/bi049753e

Liu, C.-Y., Hung, M.-H., Wang, D.-S., Chu, P.-Y., Su, J.-C., Teng, T.-H., Huang, C.-T., Chao, T.-T., Wang, C.-Y., Shiau, C.-W., Tseng, L.-M., Chen, K.-F., 2014. Tamoxifen induces apoptosis through cancerous inhibitor of protein phosphatase 2A–dependent phospho-Akt inactivation in estrogen receptor–negative human breast cancer cells. Breast Cancer Res. 16, 431. doi:10.1186/s13058-014-0431-9

Lu, K.P., Lu, K.P., Finn, G., Finn, G., Lee, T.H., Lee, T.H., Nicholson, L.K., Nicholson, L.K., 2007. Isomerization As a Molecular Timer. Nat. Chem. Biol. 3, 1–11.

doi:10.1038/nchembioYYY

Lu, K.P., Zhou, X.Z., 2007. The prolyl isomerase PIN1: a pivotal new twist in phosphorylation signalling and disease. Nat. Rev. Mol. Cell Biol. 8, 904–916. doi:10.1038/nrm2261

Manning, B.D., Cantley, L.C., 2007. AKT/PKB Signaling: Navigating Downstream. Cell. doi:10.1016/j.cell.2007.06.009

Mendoza, M.C., Er, E.E., Blenis, J., 2011. The Ras-ERK and PI3K-mTOR pathways: cross-talk and compensation. Trends Biochem. Sci. 36, 320–328. doi:10.1016/j.tibs.2011.03.006

Park, H.S., Jang, M.H., Kim, E.J., Kim, H.J., Lee, H.J., Kim, Y.J., Kim, J.H., Kang, E., Kim, S.-W., Kim, I.A., Park, S.Y., 2014. High EGFR gene copy number predicts poor outcome in triple-negative breast cancer. Mod. Pathol. 27, 1212–22. doi:10.1038/modpathol.2013.251

Pinton, P., Rimessi, A., Marchi, S., Orsini, F., Migliaccio, E., Giorgio, M., Contursi, C., Minucci, S., Mantovani, F., Wieckowski, M.R., Del Sal, G., Pelicci, P.G., Rizzuto, R., 2007. Protein kinase C beta and prolyl isomerase 1 regulate mitochondrial effects of the life-span determinant p66Shc. Science 315, 659–663. doi:10.1126/science.1135380

Rajendran, M., Thomes, P., Zhang, L., Veeramani, S., Lin, M.-F., 2010. p66Shc--a longevity redox protein in human prostate cancer progression and metastasis : p66Shc in cancer progression and metastasis. Cancer Metastasis Rev. 29, 207–22. doi:10.1007/s10555-010-9213-8

Ranganathan, R., Lu, K.P., Hunter, T., Noel, J.P., 1997. Structural and functional analysis of the mitotic rotamase Pin1 suggests substrate recognition is phosphorylation dependent. Cell 89, 875–886. doi:10.1016/S0092-8674(00)80273-1

Roberts, P.J., Der, C.J., 2007. Targeting the Raf-MEK-ERK mitogen-activated protein kinase cascade for the treatment of cancer. Oncogene 26, 3291–310.

doi:10.1038/sj.onc.1210422

Roshan, B., Kjelsberg, C., Spokes, K., Eldred, A., Crovello, C.S., Cantley, L.G., 1999. Activated ERK2 interacts with and phosphorylates the docking protein GAB1. J. Biol. Chem. 274, 36362–36368. doi:10.1074/jbc.274.51.36362

Seet, B.T., Dikic, I., Zhou, M.-M., Pawson, T., 2006. Reading protein modifications with interaction domains. Nat. Rev. Mol. Cell Biol. 7, 473–483. doi:10.1038/nrm1960

Seshacharyulu, P., Pandey, P., Datta, K., Batra, S.K., 2013. Phosphatase: PP2A structural importance, regulation and its aberrant expression in cancer. Cancer Lett. doi:10.1016/j.canlet.2013.02.036

Soule, H.D., Maloney, T.M., Wolman, S.R., Peterson, W.D.J., Brenz, R., McGrath, C.M., Russo, J., Pauley, R.J., Jones, R.F., Brooks, S.C., 1990. Isolation and characterization of a spontaneously immortalized human breast epithelial cell line, MCF-10. Cancer Res. 50, 6075–86.

Suen, K.M., Lin, C.-C., George, R., Melo, F.A., Biggs, E.R., Ahmed, Z., Drake, M.N., Arur, S., Arold, S.T., Ladbury, J.E., 2013. Interaction with Shc prevents aberrant Erk activation in the absence of extracellular stimuli. Nat. Struct. Mol. Biol. doi:10.1038/nsmb.2557

Suen, K.M., Lin, C.-C., George, R., Melo, F. a, Biggs, E.R., Ahmed, Z., Drake, M.N., Arur, S., Arold, S.T., Ladbury, J.E., 2013. Interaction with Shc prevents aberrant Erk activation in the absence of extracellular stimuli. Nat. Struct. Mol. Biol. 20, 620–7. doi:10.1038/nsmb.2557

Suenaga, A., Hatakeyama, M., Kiyatkin, A.B., Radhakrishnan, R., Taiji, M., Kholodenko, B.N., 2009. Molecular dynamics simulations reveal that Tyr-317 phosphorylation reduces Shc binding affinity for phosphotyrosyl residues of epidermal growth factor receptor.

Biophys. J. 96, 2278–2288. doi:10.1016/j.bpj.2008.11.018

Suenaga, A., Kiyatkin, A.B., Hatakeyama, M., Futatsugi, N., Okimoto, N., Hirano, Y., Narumi, T., Kawai, A., Susukita, R., Koishi, T., Furusawa, H., Yasuoka, K., Takada, N., Ohno, Y., Taiji, M., Ebisuzaki, T., Hoek, J.B., Konagaya, A., Kholodenko, B.N., 2004. Tyr-317 Phosphorylation Increases Shc Structural Rigidity and Reduces Coupling of Domain Motions Remote from the Phosphorylation Site as Revealed by Molecular Dynamics Simulations. J. Biol. Chem. 279, 4657–4662. doi:10.1074/jbc.M310598200

Ursini-Siegel, J., Hardy, W.R., Zheng, Y., Ling, C., Zuo, D., Zhang, C., Podmore, L., Pawson, T., Muller, W.J., 2012. The ShcA SH2 domain engages a 14-3-3/PI3'K signaling complex and promotes breast cancer cell survival. Oncogene 31, 5038–5044. doi:10.1038/onc.2012.4

Ursini-Siegel, J., Muller, W.J., 2008. The ShcA adaptor protein is a critical regulator of breast cancer progression. Cell Cycle 7, 1936–1943. doi:6205 [pii]

Vanhaesebroeck, B., Stephens, L., Hawkins, P., 2012. PI3K signalling: the path to discovery and understanding. Nat. Rev. Mol. Cell Biol. 13, 195–203. doi:10.1038/nrm3290

Wills, M.K.B., Jones, N., 2012. Teaching an old dogma new tricks: twenty years of Shc adaptor signalling. Biochem. J 447, 1–16. doi:10.1042/BJ20120769

Wu, Y., Chen, Z., Ullrich, A., 2003. EGFR and FGFR signalling through FRS2 is subject to negative feedback control by ERK1/2. Biol. Chem. 384, 1215–1226. doi:10.1515/BC.2003.134

Yaffe, M.B., Elia, A.E.H., 2001. Phosphoserine/threonine-binding domains. Curr. Opin. Cell Biol. doi:10.1016/S0955-0674(00)00189-7

Yu, C.F., Liu, Z.X., Cantley, L.G., 2002. ERK negatively regulates the epidermal growth factor-

mediated interaction of Gab1 and the phosphatidylinositol 3-kinase. J. Biol. Chem. 277, 19382–19388. doi:10.1074/jbc.M200732200

Yu, C.F., Roshan, B., Liu, Z.X., Cantley, L.G., 2001. ERK Regulates the Hepatocyte Growth Factor-mediated Interaction of Gab1 and the Phosphatidylinositol 3-Kinase. J. Biol. Chem. 276, 32552–32558. doi:10.1074/jbc.M104493200

Zheng, Y., Zhang, C., Croucher, D.R., Soliman, M. a, St-Denis, N., Pasculescu, A., Taylor, L., Tate, S. a, Hardy, W.R., Colwill, K., Dai, A.Y., Bagshaw, R., Dennis, J.W., Gingras, A.-C., Daly, R.J., Pawson, T., 2013. Temporal regulation of EGF signalling networks by the scaffold protein Shc1. Nature 499, 166–71. doi:10.1038/nature12308

Zhou, X.Z., Kops, O., Werner, A., Lu, P.-J., Shen, M., Stoller, G., Küllertz, G., Stark, M., Fischer, G., Lu, K.P., 2000. Pin1-Dependent Prolyl Isomerization Regulates Dephosphorylation of Cdc25C and Tau Proteins. Mol. Cell 6, 873–883. doi:10.1016/S1097-2765(05)00083-3

Funding: SKM was supported by the Rosalie B. Hite Fellowship

Acknowledgements: We are grateful to Dr. David Hawke for his assistance in proteomics analysis.

Author Contributions: SKM and CCL designed and performed experiments, analysed data and helped with manuscript preparation. CS, RG, GP-M, ABB, ZA and STA designed and performed experiments and contributed to data analysis. JEL designed experiments and wrote the manuscript. All authors reviewed the manuscript.

Competing Financial Interests: None of the contributing authors have any competing financial interests associated with this study.

Figure 1

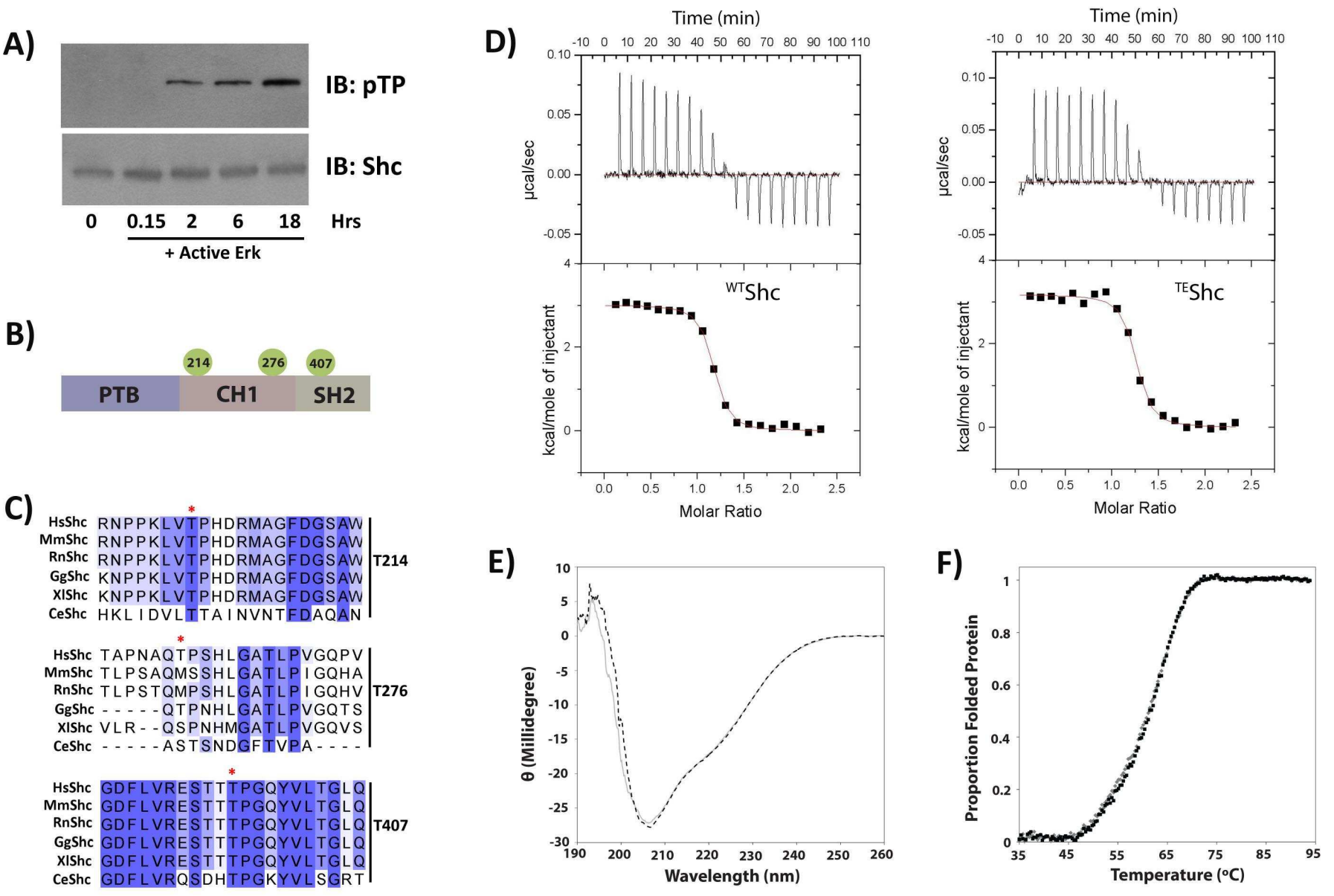
A)
IB: pTP
IB: Shc
0
0.15
2
6
18
Hrs
+ Active Erk
B)
214
276
407
PTB
CH1
SH2
C)
HsShc RNPPKLVTPHDRMAGFDGSAW
MmShc RNPPKLVTPHDRMAGFDGSAW
RnShc RNPPKLVTPHDRMAGFDGSAW
GgShc KNPPKLVTPHDRMAGFDGSAW
XlShc KNPPKLVTPHDRMAGFDGSAW
CeShc HKLIDVLTTAINVNTFDAQAN
T214
HsShc TAPNAQTPSHLGATLPVGQPV
MmShc TLPSAQMSSHLGATLPIGQHA
RnShc TLPSTQMPSHLGATLPIGQHV
GgShc -----QTPNHLGATLPVGQTS
XlShc VLR--QSPNHMGATLPVGQVS
CeShc -----ASTSNDGFTVPA----
T276
HsShc GDFLVRESTTTPGQYVLTGLQ
MmShc GDFLVRESTTTPGQYVLTGLQ
RnShc GDFLVRESTTTPGQYVLTGLQ
GgShc GDFLVRESTTTPGQYVLTGLQ
XlShc GDFLVRESTTTPGQYVLTGLQ
CeShc GDFLVRQSDHTPGKYVLSGRT
T407
D)
Time (min)
µcal/sec
kcal/mole of injectant
WTShc
TEShc
Molar Ratio
E)
θ (Millidegree)
Wavelength (nm)
F)
Proportion Folded Protein
Temperature (°C)

Figure 2

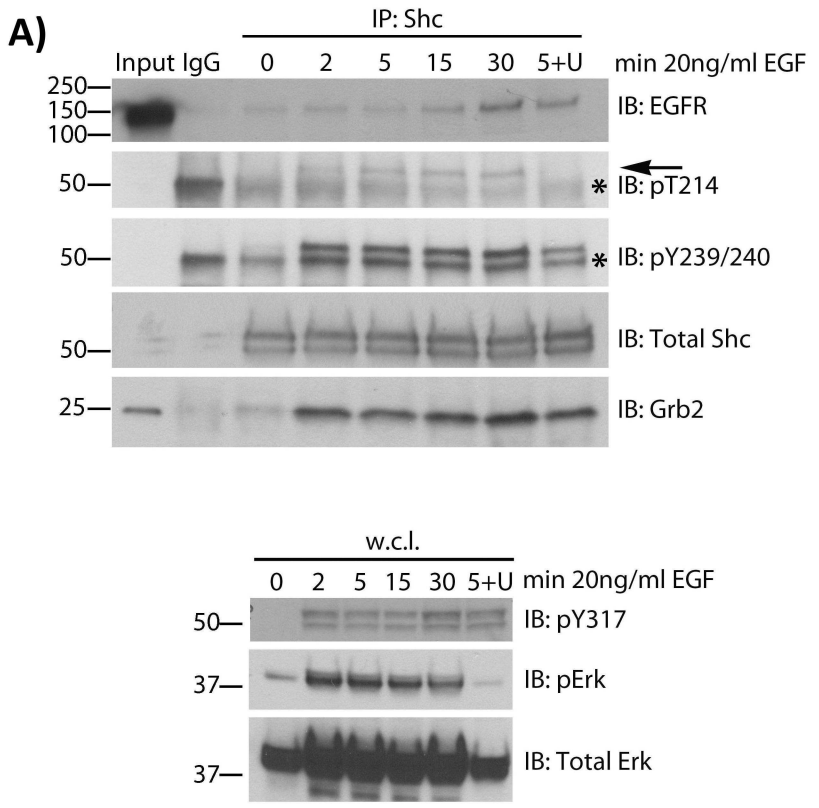
A)
IP: Shc
Input IgG 0 2 5 15 30 5+U min 20ng/ml EGF
250
150
100
IB: EGFR
50
IB: pT214
50
IB: pY239/240
50
IB: Total Shc
25
IB: Grb2
w.c.l.
0 2 5 15 30 5+U min 20ng/ml EGF
50
IB: pY317
37
IB: pErk
37
IB: Total Erk

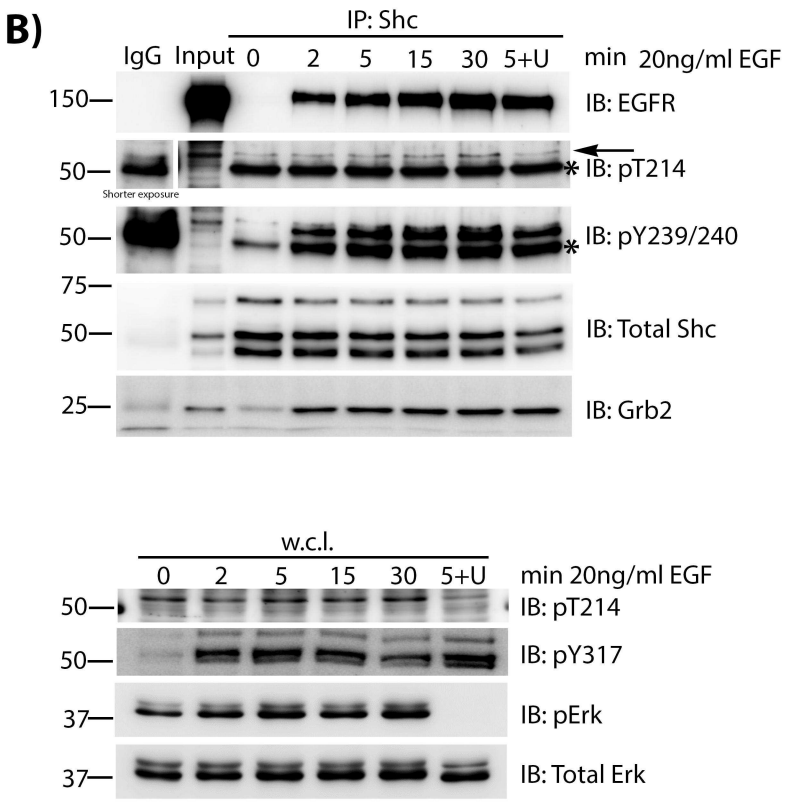
B)
IP: Shc
IgG Input 0 2 5 15 30 5+U min 20ng/ml EGF
150
IB: EGFR
50
Shorter exposure
IB: pT214
50
IB: pY239/240
75
50
IB: Total Shc
25
IB: Grb2
w.c.l.
0 2 5 15 30 5+U min 20ng/ml EGF
50
IB: pT214
50
IB: pY317
37
IB: pErk
37
IB: Total Erk

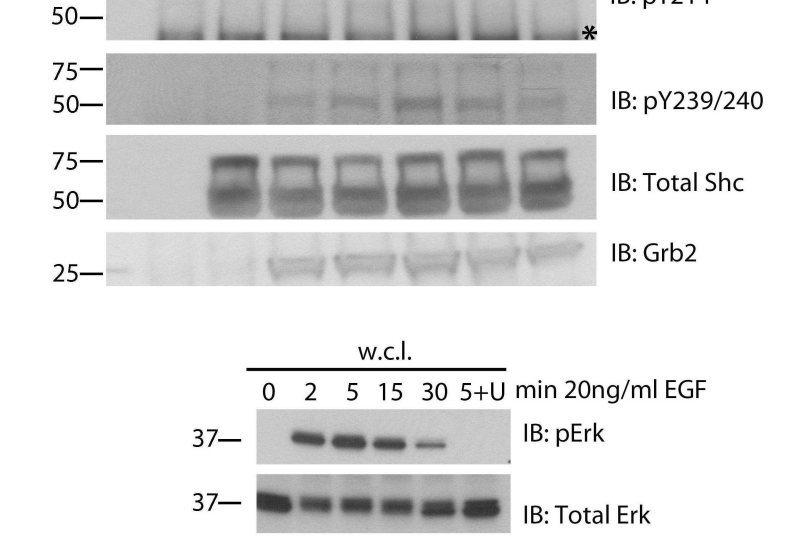
C)
IP: Shc
Input IgG 0 2 5 15 30 5+U min 20ng/ml EGF
250
150
100
IB: EGFR
75
50
IB: pT214
75
50
IB: pY239/240
75
50
IB: Total Shc
25
IB: Grb2
w.c.l.
0 2 5 15 30 5+U min 20ng/ml EGF
37
IB: pErk
37
IB: Total Erk

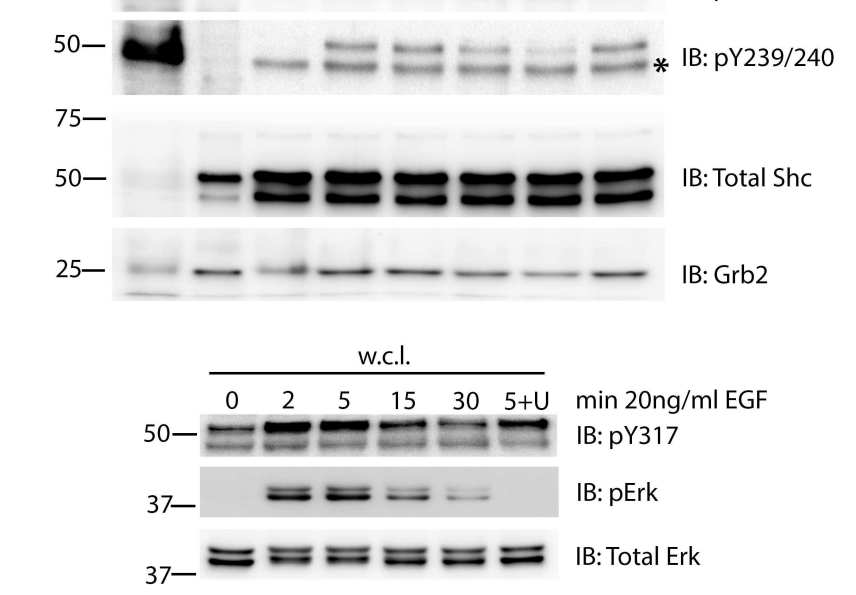
D)
IP: Shc
IgG Input 0 2 5 15 30 5+U min 20ng/ml EGF
150
IB: EGFR
50
IB: pT214
50
IB: pY239/240
75
50
IB: Total Shc
25
IB: Grb2
w.c.l.
0 2 5 15 30 5+U min 20ng/ml EGF
50
IB: pY317
37
IB: pErk
37
IB: Total Erk

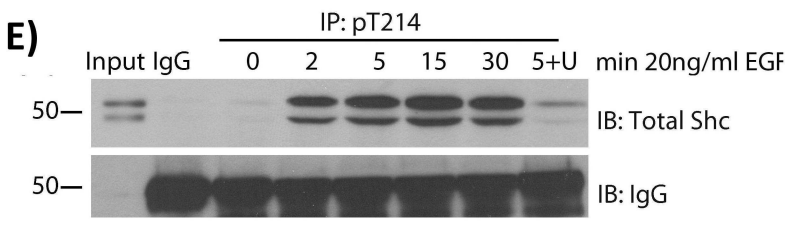
E)
IP: pT214
Input IgG 0 2 5 15 30 5+U min 20ng/ml EGF
50
IB: Total Shc
50
IB: IgG

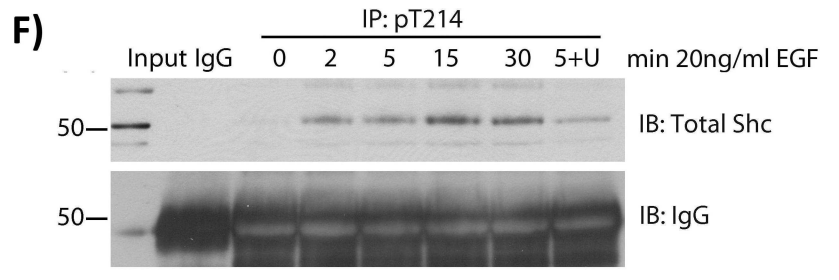
F)
IP: pT214
Input IgG 0 2 5 15 30 5+U min 20ng/ml EGF
50
IB: Total Shc
50
IB: IgG

Figure 3

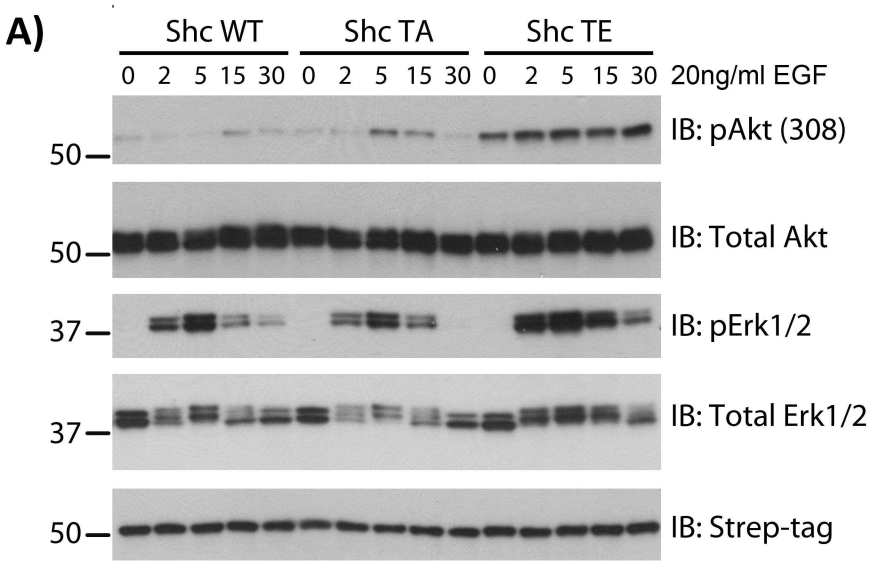
A)
Shc WT
Shc TA
Shc TE
0 2 5 15 30 0 2 5 15 30 0 2 5 15 30 20ng/ml EGF
50
IB: pAkt (308)
50
IB: Total Akt
37
IB: pErk1/2
37
IB: Total Erk1/2
50
IB: Strep-tag

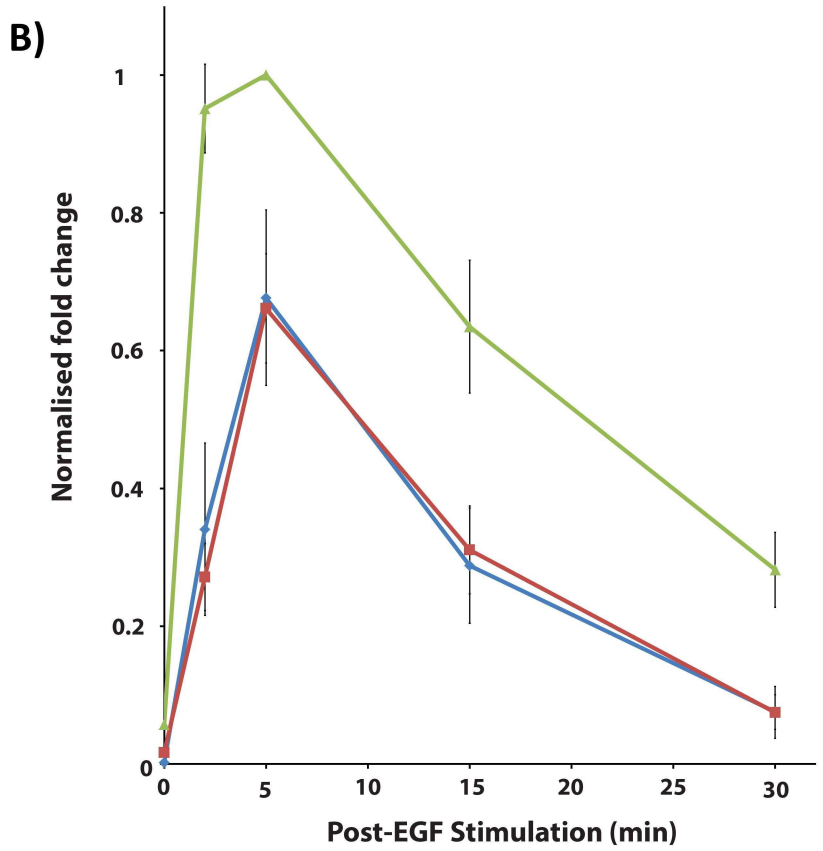
B)
Normalised fold change
0
0.2
0.4
0.6
0.8
1
0 5 10 15 20 25 30
Post-EGF Stimulation (min)

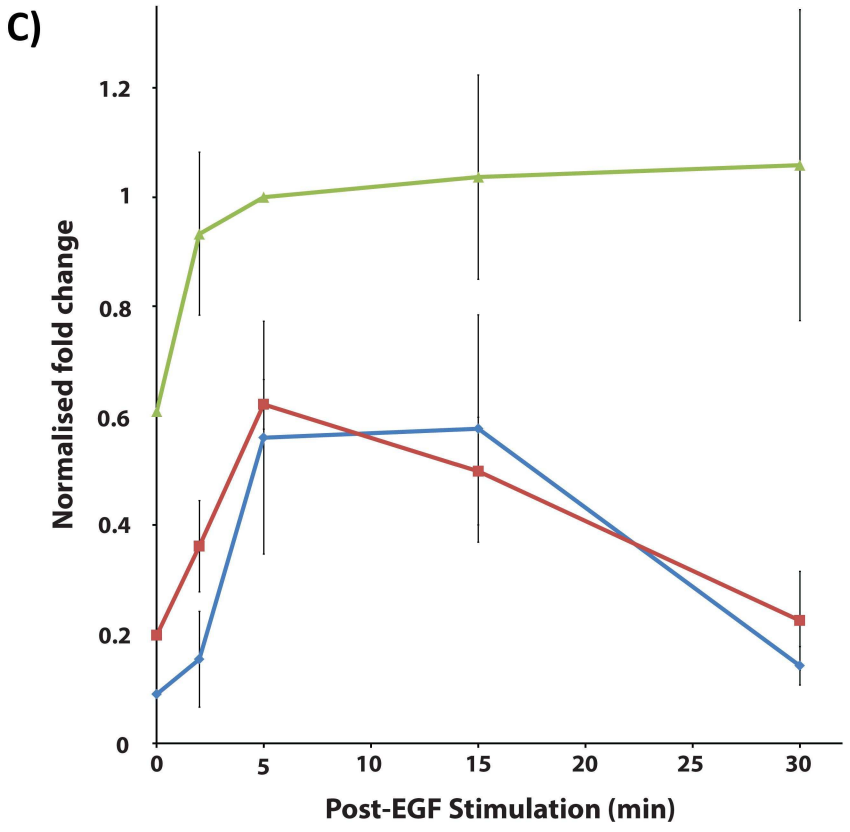
C)
Normalised fold change
0
0.2
0.4
0.6
0.8
1
1.2
0 5 10 15 20 25 30
Post-EGF Stimulation (min)

Figure 4

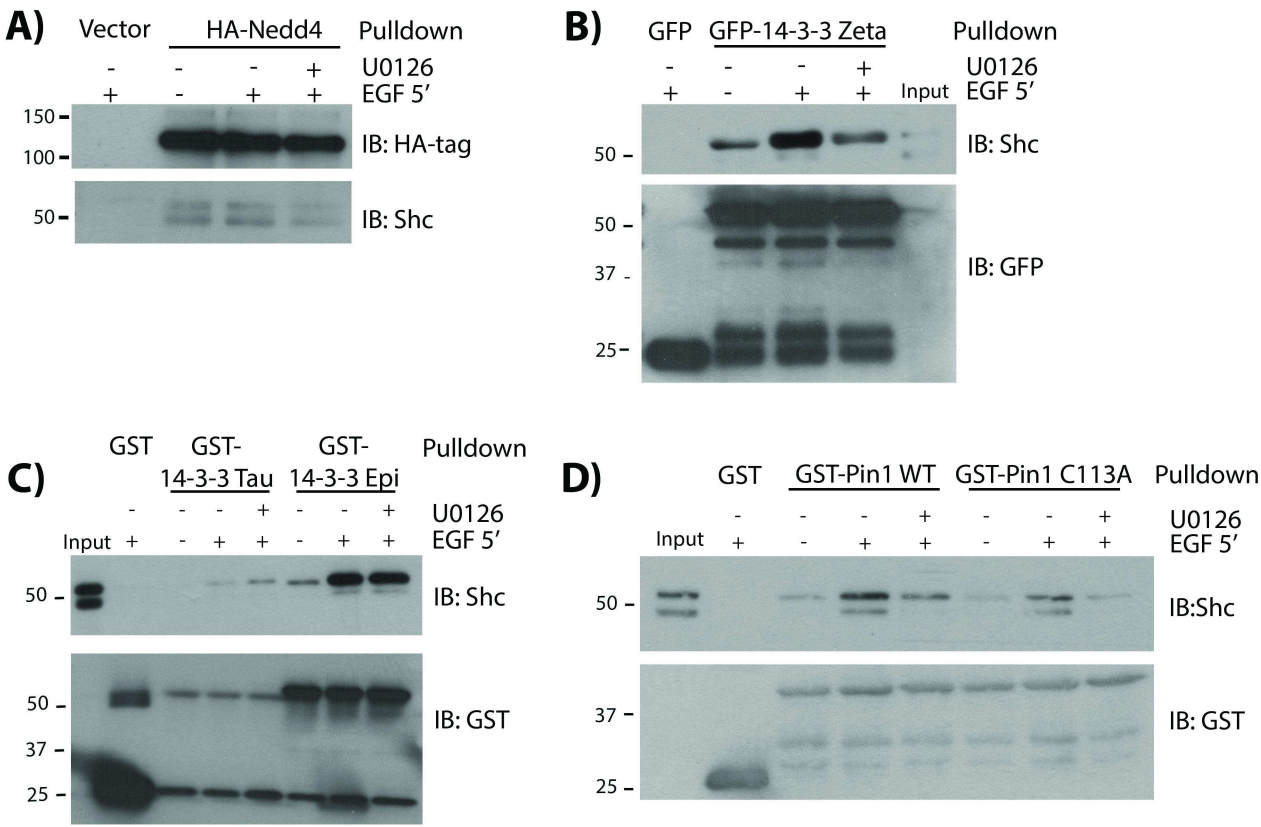
A)
Vector
HA-Nedd4
Pulldown
U0126
EGF 5′
150
100
IB: HA-tag
50
IB: Shc
B)
GFP
GFP-14-3-3 Zeta
Pulldown
U0126
Input
EGF 5′
50
IB: Shc
50
37
25
IB: GFP
C)
GST
GST-14-3-3 Tau
GST-14-3-3 Epi
Pulldown
U0126
Input
EGF 5′
50
IB: Shc
50
37
25
IB: GST
D)
GST
GST-Pin1 WT
GST-Pin1 C113A
Pulldown
U0126
Input
EGF 5′
50
IB:Shc
37
25
IB: GST

Figure 5

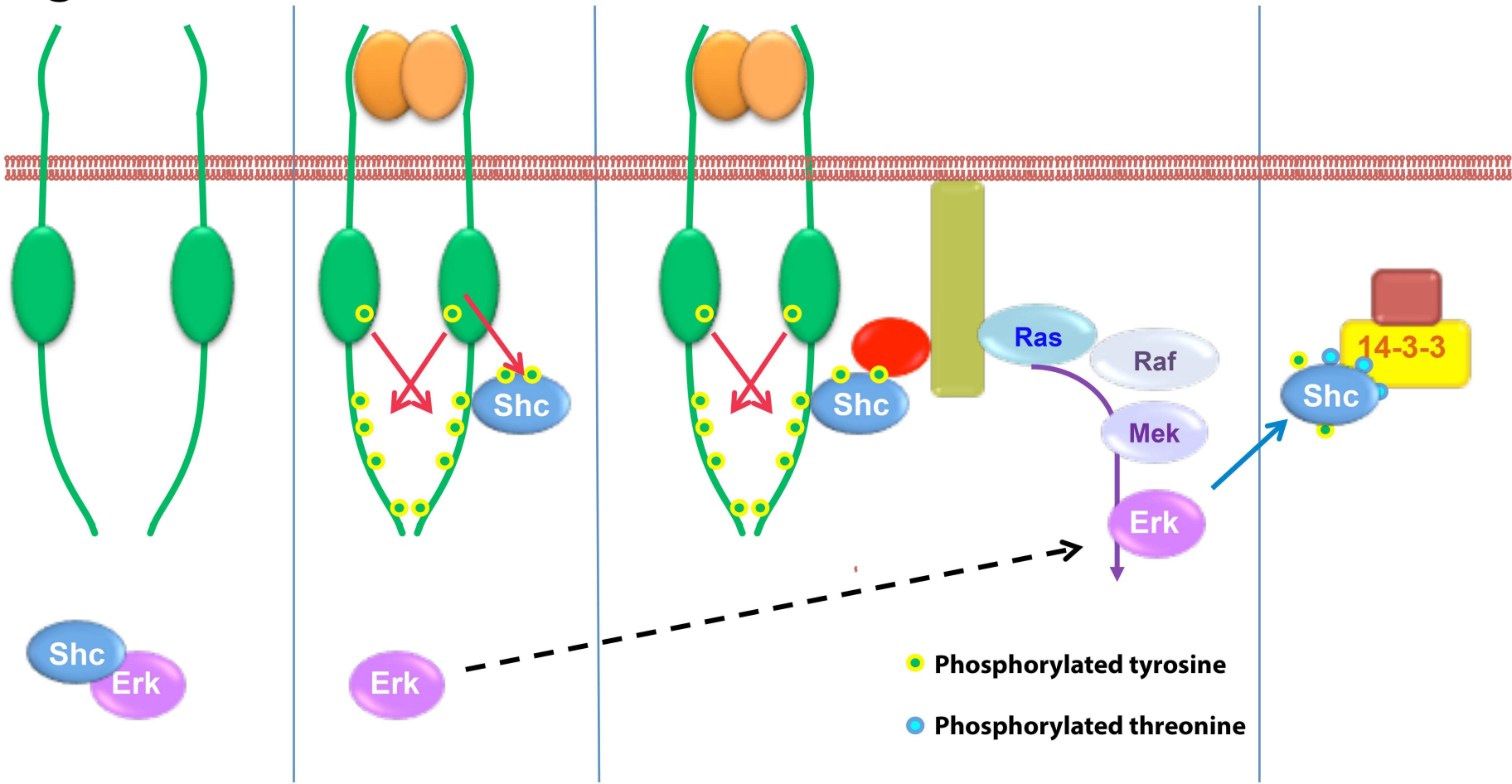
Shc
Erk
Shc
Erk
Shc
Ras
Raf
Mek
Erk
14-3-3
Shc
Phosphorylated tyrosine
Phosphorylated threonine